

GMODiff: One-Step Gain Map Refinement with Diffusion Priors for HDR Reconstruction

Tao Hu¹ Weiyu Zhou¹ Yanjie Tu¹ Peng Wu¹ Wei Dong²
Qingsen Yan^{1*} Yanning Zhang¹

¹Northwestern Polytechnical University ²Xi’an University of Architecture and Technology

Abstract

Pre-trained Latent Diffusion Models (LDMs) have recently shown strong perceptual priors for low-level vision tasks, making them a promising direction for multi-exposure High Dynamic Range (HDR) reconstruction. However, directly applying LDMs to HDR remains challenging due to: (1) limited dynamic-range representation caused by 8-bit latent compression, (2) high inference cost from multi-step denoising, and (3) content hallucination inherent to generative nature. To address these challenges, we introduce GMODiff, a gain map-driven one-step diffusion framework for multi-exposure HDR reconstruction. Instead of reconstructing full HDR content, we reformulate HDR reconstruction as a conditionally guided Gain Map (GM) estimation task, where the GM encodes the extended dynamic range while retaining the same bit depth as LDR images. We initialize the denoising process from an informative regression-based estimate rather than pure noise, enabling the model to generate high-quality GMs in a single denoising step. Furthermore, recognizing that regression-based models excel in content fidelity while LDMs favor perceptual quality, we leverage regression priors to guide both the denoising process and latent decoding of the LDM, suppressing hallucinations while preserving structural accuracy. Extensive experiments demonstrate that our GMODiff performs favorably against several state-of-the-art methods and is 100× faster than previous LDM-based methods.

1. Introduction

Multi-exposure High Dynamic Range (HDR) imaging fuses Low Dynamic Range (LDR) images of varying exposures to recover scene radiance, but suffers from motion-induced misalignment in dynamic scenes. Recent Deep Neural Networks (DNNs), including Convolutional Neural Networks (CNNs) and Vision Transformers (ViTs) [18, 24, 34, 38,

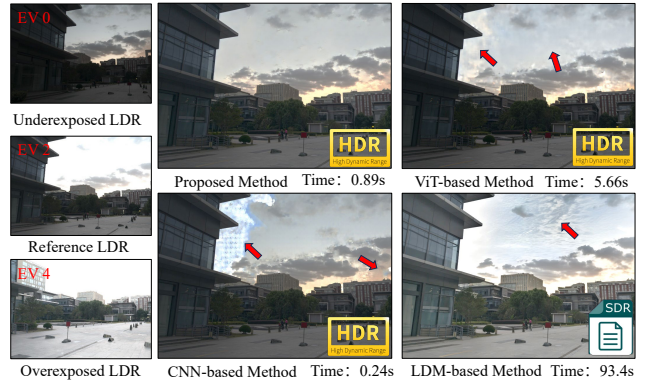


Figure 1. Compared to DNN-based methods, LDM-based method generates perceptually compelling HDR-like images, demonstrating their potential for HDR reconstruction. However, they suffer from high computational overhead and are prone to hallucination artifacts that compromise physical fidelity.

41–43], have greatly improved HDR reconstruction in dynamic scenes. Despite their advancements, these methods simply learn a mapping network between LDR-HDR paired data using pixel-wise losses [36], which often yields perceptually unsatisfactory results. This limitation is particularly pronounced when essential content is missing in severely overexposed regions due to object or camera motion.

Recent advances in Latent Diffusion models (LDMs) [9, 14, 33], particularly large-scale pre-trained text-to-image (T2I) models [29–31] trained on billions of image-text pairs, possess powerful natural image priors. These priors make LDMs a promising solution for addressing the perceptual shortcomings of current HDR reconstruction methods, especially in mitigating motion-induced ghosting and other complex artifacts. However, directly applying LDMs to high-quality HDR image generation remains non-trivial due to three key challenges: **(1) Limited Dynamic Range Representation:** The autoencoders of pre-trained LDMs compress linear HDR distributions into an 8-bit perceptual latent space, limiting their capacity to represent the dynamic range of HDR content [13, 35]. **(2) High Inference Cost:**

*Corresponding author.

LDMs demand a substantial number of iteration steps in the denoising process, which is time-consuming even with a high-end GPU card [17, 45]. **(3) Content Hallucination:** The generative nature of LDMs can lead to hallucinated content that deviates from realistic scenes. As shown in Fig. 1, UltraFusion [8] produces human-perceptually consistent HDR-like content with a compressed dynamic range but suffer from high latency and hallucination.

These limitations motivate a paradigm shift in leveraging LDMs for HDR reconstruction. Our work draws from three key insights: **First**, inspired by the observation that an HDR image can be decomposed into a LDR component and a 8 bit-depth Gain Map (GM) [1, 2, 12] that encodes the extended dynamic range, we reframe HDR reconstruction as a conditionally guided GM estimation task to fully exploit pre-trained LDM priors without domain mismatches. **Second**, since LDR inputs already provide rich structural and semantic cues, we initialize the denoising process from an informative prior (*e.g.*, a regression-based GM estimate) rather than pure noise, significantly accelerating inference. **Third**, recognizing that regression-based models excel in content fidelity while LDMs favor perceptual quality, we leverage regression-based priors to guide the LDM’s denoising and latent decoding processes.

Building on these principles, we propose GModiff, a gain map-driven one-step diffusion model for multi-exposure HDR reconstruction. Rather than training a LDM to directly reconstruct full HDR content, we adopt a two-stage fine-tuning strategy to adapt a pre-trained multi-step LDM for single-step GM refinement. Specifically, in the first stage, we train a Degradation-aware Regressor Network (DaReg) via a dual-learning strategy to produce an initial GM and extract spatial embeddings that highlight regions where the estimate is unreliable. This joint learning scheme provides the LDM with an informative prior for initialization and directs its attention to ambiguous or error-prone areas, significantly accelerating convergence and improving structural fidelity. In the second stage, we fine-tune the LDM to perform one-step denoising conditioned on these regression-based priors, enabling accurate GM correction and high-fidelity HDR reconstruction at dramatically reduced computational cost. In summary, our main contributions are threefold:

- We propose GModiff, a one-step diffusion framework that reframes HDR reconstruction as a conditionally guided gain map refinement task, fully leveraging pre-trained LDMs without redesigning the latent space.
- We design a unified prior-guided refinement pipeline that seamlessly integrates regression-based fidelity with diffusion-driven perceptual enhancement: the DaReg produces an initial gain map and degradation-aware embeddings, which guide both the denoising process and the latent decoding of the LDM, effectively suppressing hal-

lucinations while preserving structural accuracy.

- Extensive experiments demonstrate that the proposed GModiff delivers superior visual quality with significantly reduced ghosting and artifacts, while achieving high inference efficiency.

2. Related Work

2.1. Multi-exposure HDR Reconstruction

Multi-exposure HDR imaging has advanced significantly, with methods broadly divided into traditional and deep learning-based categories. Traditional methods address motion artifacts via motion rejection [11], registration [4, 19], and patch matching [16, 32], but their effectiveness hinges on preprocessing accuracy, often failing with large/complex motion. In contrast, state-of-the-art HDR reconstruction methods now predominantly leverage the powerful non-linear modeling capabilities of DNNs. Recent advances incorporate attention mechanisms [6, 41, 43] and ViT architectures [24, 34, 43] to improve feature correspondence and capture long-range dependencies. Meanwhile, optical flow-guided approaches [18, 20] explicitly address misalignment by warping input frames according to estimated motion fields. Moreover, generative models, including Generative Adversarial Networks (GANs) [27] and diffusion models [8, 17, 35, 45], have been successfully adapted to synthesize photorealistic HDR content, even from imperfect or severely degraded inputs. Additional innovative frameworks, such as [13, 22, 23, 26], have further expanded the scope of DNN applications in this field, introducing novel architectures and training strategies to improve reconstruction quality. Despite these advances, most existing methods either learn a direct LDR-to-HDR mapping using pixel-wise losses, or train generative models from scratch on limited datasets. These often yield unsatisfactory results, especially when critical content is missing in severely over/underexposed regions due to motion.

2.2. Diffusion Models

Diffusion models have emerged as a powerful class of generative frameworks, capable of synthesizing high-fidelity data through iterative denoising of random noise. They have already demonstrated impressive performance across a wide range of low-level vision tasks—such as super-resolution [5, 46], denoising [10], image enhancement [21], colorization [10], and deblurring [39], thanks to their ability to model fine-grained details and generate visually compelling outputs, often surpassing traditional image restoration methods. Despite their success, the practical deployment of diffusion models remains hindered by their high computational cost, which arises from both complex network architectures [25, 33] and the requirement for hundreds of iterative sampling steps during inference. To mit-

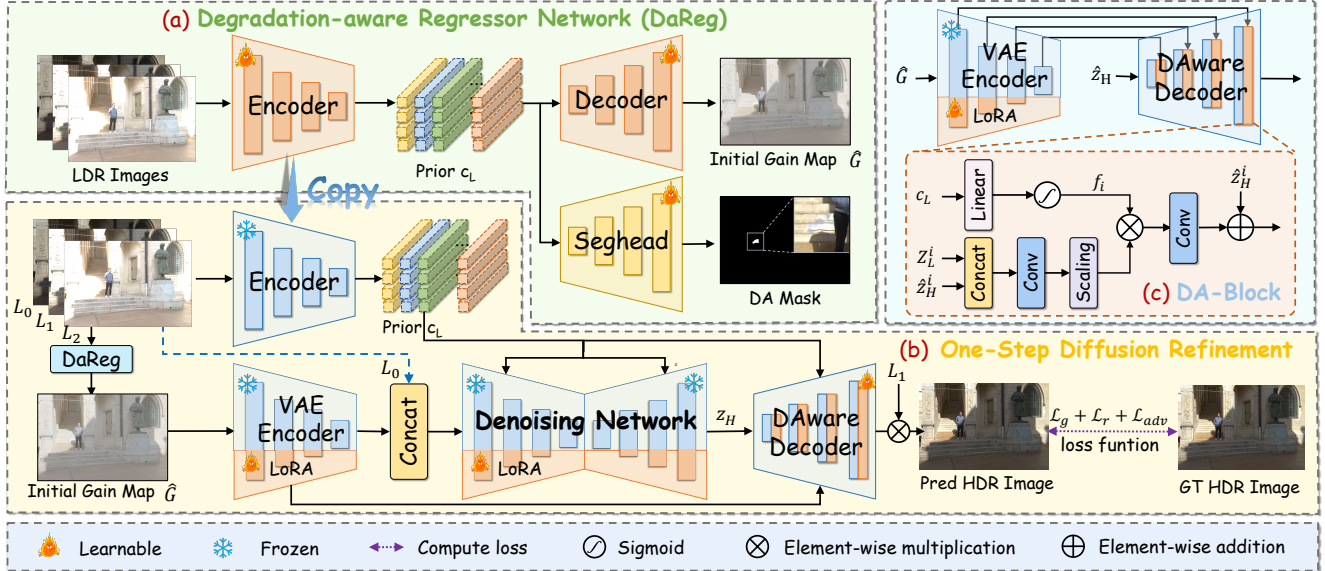


Figure 2. Overview of the proposed GModiff framework. (a) We train a DaReg via a dual-learning strategy to produce two regression-based priors: an initial gain map \hat{G} and spatial embeddings c_L . The c_L implicitly encode regions where the \hat{G} is unreliable, serving as a degradation-aware guidance prior. (b) One-Step Diffusion Refinement initializes the denoising process from \hat{G} and performs single-step denoising conditioned on c_L to generate a high-fidelity GM latent code z_H . (c) The DA Decoder leverages encoder features from the initial gain map \hat{G} , guided by c_L , to recover fine image details while avoiding the introduction of artifacts inherent in \hat{G} .

igate this bottleneck, recent efforts have focused on accelerating diffusion by drastically reducing the number of denoising steps. However, aggressive step reduction typically leads to a noticeable degradation in output quality. Recently, img2img [28] proposed a general framework that adapts pre-trained single-step diffusion models [37, 40] to new tasks and domains via adversarial learning. This approach enables efficient inference while leveraging the rich internal knowledge embedded in large-scale pre-trained diffusion models. Nevertheless, directly applying this efficient diffusion paradigm to HDR generation remains challenging. Most pre-trained diffusion models rely on autoencoders trained on 8-bit LDR images, which compress HDR’s high bit-depth into a perceptually encoded, low-dimensional latent space, severely limiting their ability to capture the full dynamic range of the real world.

3. Methodology

As shown in Fig. 2, GModiff is trained in two stages. During the first stage (Sec. 3.2), we pretrain a Degradation-aware Regressor Network (DaReg) to predict an initial gain map and degradation-aware embeddings from the LDR inputs. During the second stage (Sec. 3.3), we fine-tune a pre-trained LDM using these regression priors to refine the initial gain map and reconstruct a high-quality HDR image.

3.1. Preliminaries

As shown in Fig. 3 (a), while the variational autoencoder (VAE) of a LDM can encode visually plausible LDR repre-

sentations that resemble HDR content under standard viewing conditions, it fundamentally fails to preserve true high dynamic range—particularly in highlights and shadows. Moreover, since the denoising network operates in an 8-bit perceptual latent space, a naive solution to enable HDR generation would be to fine-tune both the VAE and the denoising network on HDR data. However, this approach demands large-scale HDR training sets and discards the rich generative priors learned from massive LDR images [35].

Recent advances in display technology have popularized dual-layer HDR formats [2, 12], which decompose an HDR image \mathbf{H} into an LDR base layer \mathbf{L} and an 8-bit gain map \mathbf{G} . The gain map is obtained by pixel-wise division of \mathbf{H} by \mathbf{L} , followed by logarithmic compression. As shown in Fig. 3 (b), the original HDR image can then be reconstructed as:

$$\mathbf{H} = (\mathbf{L} + \alpha) \cdot \exp_2(1 + \mathbf{G} \cdot Q_{\max}), \quad (1)$$

where $\mathbf{G} \in [0, 1]$ is the normalized gain map, $\exp_2(\cdot)$ denotes the inverse log transform, Q_{\max} corresponds to the maximum gain value, and $\alpha = 1/64$ is a scaling constant that preserves detail in near-black regions. Crucially, both LDR image and gain map are 8-bit depth, allowing us to directly exploit pre-trained LDMs without VAE retraining or latent space redesign.

3.2. Degradation-aware Regressor Network

The first stage produces two regression-based priors: an initial gain map \hat{G} and multi-scale spatial embeddings c_L . These priors are used to initialize and condition the one-step

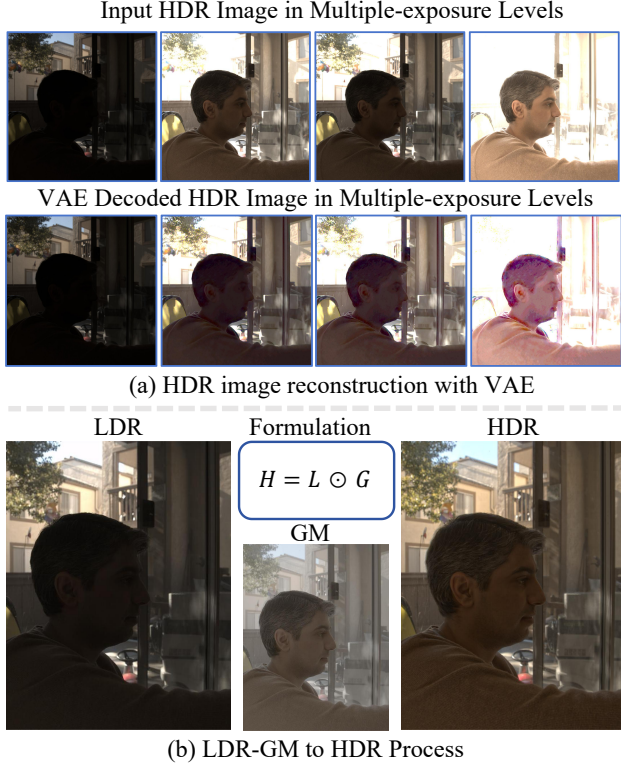


Figure 3. (a) Limitations of the vanilla LDMs in generating HDR content. The limitation of the LDM VAE in encoding and decoding an HDR image, visualized in multiple exposure levels, which reveals a significant fidelity loss, especially in the shadow. (b) The GM encodes pixel-wise dynamic range adjustments for the LDR image and can be used to reconstruct the HDR image via element-wise multiplication.

diffusion refinement, ensuring high structural fidelity while enabling perceptual enhancement.

Overall Architecture. Our DaReg adopts a NAFNet backbone [7] augmented with a lightweight degradation-aware segmentation head. Given the input LDR sequence $\{L_1, L_2, \dots, L_N\}$, we first apply gamma correction to each L_i to obtain its HDR version H_i , and form a six-channel tensor $X_i = [L_i, H_i]$ by channel-wise concatenation. Following [24, 41, 44], an implicit alignment module [41] processes the LDR inputs and fuses multi-exposure features before feeding them into the network. As shown in Fig. 2, DaReg encodes these features into multi-scale spatial embeddings:

$$\mathbf{c}_L = \{\mathbf{c}_{L_k} \in \mathbb{R}^d\}_{k=1}^K, \quad (2)$$

where \mathbf{c}_L aggregates encoder features across scales and flattens them into vector representations. The decoder reconstructs the initial gain map using \mathbf{c}_L , while the segmentation head predicts a binary reliability mask for degraded regions (e.g., due to motion or saturation). This mask endows \mathbf{c}_L with awareness of uncertain areas, guiding subsequent re-

finement.

Initial GM Reconstruction. Given an input LDR sequence, the encoder extracts multi-scale features, where each stage consists of multiple Nonlinear Activation-Free Blocks [7]. The channel dimensions at the four scales are set to 64, 128, 256, and 512, respectively. A symmetric decoder then reconstructs the initial gain map $\hat{\mathbf{G}}$ as: $\hat{\mathbf{G}} = D(\mathbf{c}_L; \phi)$, where each decoder stage receives skip-connected features from the corresponding encoder stage to progressively reconstruct the initial GM.

During training, we compute the ground-truth gain map \mathbf{G} using Eq. (1), where \mathbf{L} is the reference frame of the aligned LDR sequence. To enable direct supervision with HDR images and ensure differentiability at zero, we replace the logarithmic compression with the μ -law function. Accordingly, the $\exp_2(\cdot)$ in Eq. (1) is substituted by the inverse μ -law mapping: $R(x) = \frac{e^{x \cdot \log(1+\mu)} - 1}{\mu}$, with $\mu=100$. We supervise the initial gain map prediction $\hat{\mathbf{G}}$ via an \mathcal{L}_1 regression loss:

$$\mathcal{L}_{\text{gm}} = \|\hat{\mathbf{G}} - \mathbf{G}\|_1. \quad (3)$$

Additionally, we enforce consistency between the reconstructed HDR image $\hat{\mathbf{H}}$ (from $\hat{\mathbf{G}}$) and the ground-truth \mathbf{H} :

$$\mathcal{L}_r = \left\| \mathcal{T}(\mathbf{H}) - \mathcal{T}(\hat{\mathbf{H}}) \right\|_1 + \lambda \left\| \phi_{i,j}(\mathcal{T}(\mathbf{H})) - \phi_{i,j}(\mathcal{T}(\hat{\mathbf{H}})) \right\|_1, \quad (4)$$

where $\mathcal{T}(\cdot)$ denotes the μ -law function, $\phi_{i,j}(\cdot)$ is the j -th feature map of VGG19 after the i -th max-pooling layer, and $\lambda = 1e-2$ is a weighting hyperparameter.

Degradation-Aware Embedding. By incorporating a reconstruction objective, DaReg implicitly learns regression-based priors that facilitate dynamic range expansion. To better guide the LDM in refining the initial GM, we explicitly train it to identify a degradation-aware mask, such that \mathbf{c}_L implicitly encodes regions where $\hat{\mathbf{G}}$ is unreliable. This guides the refinement process to focus on uncertain regions while avoiding hallucinating implausible details in well-reconstructed areas.

Specifically, given an input LDR sequence, we extract multi-scale latent representations with the DaReg encoder as before. For the degradation-aware mask M , we upsample all feature maps to the original resolution, concatenate them, and feed the aggregated features into a 1×1 convolutional layer to produce $\bar{\mathbf{c}}_L$. The segmentation head $h(\cdot; \phi)$ processes $\bar{\mathbf{c}}_L$ through two convolutional layers with 64 hidden channels followed by a sigmoid activation, outputs a predict mask: $\hat{M} = h(\bar{\mathbf{c}}_L; \phi)$, where $\hat{M} \in [0, 1]$ indicates the predicted degradation at pixel p . We obtain the ground-truth mask M using a simple yet effective pixel-consistency criterion:

$$M(p) = \begin{cases} 1 & \text{if } \|\mathcal{T}(\mathbf{H}(p)) - \mathcal{T}(\hat{\mathbf{H}}(p))\|_1 > \sigma, \\ 0 & \text{otherwise,} \end{cases} \quad (5)$$

where p denotes a pixel location, $\|\cdot\|_1$ averages the absolute difference across RGB channels to yield a scalar, and $\sigma = 4/255$ is a fixed threshold. This formulation is motivated by the observation that static regions yield consistent reconstructions—even with simple image blending—whereas motion or overexposure causes significant pixel-level discrepancies. The loss function adopted is the binary cross-entropy (BCE) loss between \hat{M} and M .

3.3. Prior-Guided One-Step Diffusion Refinement

In the second stage, our goal is to efficiently leverage the strong image priors of pre-trained LDMs to address degradations in the initial GM (e.g., ghosting and artifacts), thereby reconstructing high-quality HDR images.

One-step Denoising Process. Based on the prior analysis, we formulate GM refinement as a conditionally guided image-to-image denoising process, which enables the adoption of an efficient one-step denoising strategy [40] and accelerates convergence. Our GMODiff first encodes the initial GM into the latent space via an encoder E_θ , resulting in $\mathbf{Z}_L = E_\theta(\hat{\mathbf{G}})$. A single-step denoising operation $F(\mathbf{Z}_L; \mathbf{c})$ is then performed to predict the noise $\hat{\epsilon}$, which enables us to derive the estimated high-quality latent representation $\hat{\mathbf{Z}}_H$:

$$\hat{\mathbf{Z}}_H = F(\mathbf{Z}_L; \mathbf{c}) \triangleq \frac{\mathbf{Z}_L - \sqrt{1 - \bar{\alpha}_{T_L}} \varepsilon_\theta(\mathbf{Z}_L; \mathbf{c}, T)}{\sqrt{\bar{\alpha}_T}}, \quad (6)$$

where ε_θ denotes the denoising network, \mathbf{c} is the guidance condition, $T \in [0, T]$ is the predefined diffusion timestep, and $\bar{\alpha}$ represents the predefined noise schedule. Specifically, we append trainable LoRA [15] layers to the encoder E_ϕ and the diffusion network ε_ϕ , fine-tuning them into E_θ and ε_θ using our training data. The condition \mathbf{c} includes the regression prior \mathbf{c}_L and the underexposed LDR image L_0 . \mathbf{c}_L is injected into the hidden layers of the denoising network, whereas L_0 is first encoded into a feature map, then concatenated with \mathbf{Z}_L and fed into the denoising network, with the number of channels in the first convolutional layer adjusted accordingly.

Degradation-Aware Decoder. The pre-trained LDM performs denoising in a highly compressed latent space (e.g., $\mathcal{R} \in \mathbb{R}^{4 \times \frac{H}{8} \times \frac{W}{8}}$), which can result in detail distortion in generated content [12]. To address this issue, we propose a Degradation-Aware Decoder that leverages the encoder features of $\hat{\mathbf{G}}$ under the guidance of degradation-aware priors to facilitate refinement of detail while suppressing artifacts inherent in the initial GM $\hat{\mathbf{G}}$.

Specifically, we obtain multi-scale features \mathbf{Z}_L^i of the initial GM $\hat{\mathbf{G}}$ via the VAE encoder through forward propagation, while $\hat{\mathbf{Z}}_H$ is derived from a one-step diffusion process. Although the initial gain map, reconstructed via a regression approach, endows \mathbf{Z}_L^i with rich detail fidelity, it may introduce noticeable artifacts. To address this, we propose

a Degradation-Aware Refinement Block guided by the embedding \mathbf{c}_L , which leverages degradation-aware embeddings to identify unreliable regions in \mathbf{Z}_L^i . As illustrated in Fig. 2 (c), the Degradation-Aware Refinement Block first concatenates the decoder intermediate features $\hat{\mathbf{Z}}_H^i$ with \mathbf{Z}_L^i and applies a 3×3 convolution to obtain refined features $\hat{\mathbf{Z}}^i$:

$$\hat{\mathbf{Z}}^i = \text{Conv}_{3 \times 3}([\hat{\mathbf{Z}}_H^i, \mathbf{Z}_L^i]), \quad (7)$$

where $[\cdot]$ denotes channel-wise concatenation. The \mathbf{c}_L is then passed through an MLP followed by a sigmoid activation to produce a channel-wise modulation vector:

$$\begin{aligned} \mathbf{f}_i &= \text{Sigmoid}(\text{MLP}(\mathbf{c}_L)), \\ \hat{\mathbf{Z}}_H^{i+1} &= \text{Conv}_{3 \times 3}(\hat{\mathbf{Z}}^i \odot \mathbf{f}_i) + \hat{\mathbf{Z}}_H^i, \end{aligned} \quad (8)$$

where \odot denotes channel-wise multiplication, and $\hat{\mathbf{Z}}_H^{i+1}$ represents the updated decoder feature after detail modulation and residual connection.

Training Strategy During the training phase, the loss function comprises the GM reconstruction loss and HDR reconstruction loss. Following [40], we also compute the adversarial loss \mathcal{L}_{adv} between the reconstructed HDR image and the GT HDR image in the μ -law domain. The total objective for decoder training is:

$$\mathcal{L}_{diff} = \mathcal{L}_{gm} + \mathcal{L}_r + \lambda \mathcal{L}_{adv} \quad (9)$$

where λ denotes the balancing parameter, which is empirically set to 0.001.

Additionally, considering that the initial GM $\hat{\mathbf{G}}$ obtained in the first stage may overfit to the training set, which impairs GMODiff’s ability to handle its degradations, we propose a group training strategy for GMODiff to learn robust degradation mitigation. Specifically, we divide the training set into N groups and train $N + 1$ DaRegs accordingly, with the extra model trained on the entire training dataset. During GMODiff training, we randomly select one DaReg to provide $\hat{\mathbf{G}}$ and \mathbf{c}_L . The training objective for GMODiff is ultimately defined as the expected loss over such random selections:

$$\mathcal{L} = \mathbb{E}k \sim \text{Uniform}(0, N) \left[\mathcal{L}_{diff} \left(\hat{\mathbf{G}}_k, \mathbf{c}_{L,k}; H; G \right) \right] \quad (10)$$

where k is the index of a randomly selection.

4. Experiments

4.1. Experimental Settings

Datasets. We collect publicly available real-world datasets commonly used for multi-exposure HDR reconstruction from multiple sources [18, 20, 34], resulting in a total of 836 image pairs. Among these, 758 pairs are used for training and the remaining 78 for testing. Each sample consists

Table 1. Quantitative comparison across methods. Higher (\uparrow) is better for PU-PSNR, PU-SSIM, MANIQA, MUSIQ, CLIPIQA; lower (\downarrow) is better for LPIPS, DISTs, and NIQE. Best and second-best results per metric are highlighted in red and blue, respectively.

Metric	DeepHDR [38]	NHDRR [42]	AHDRNet [41]	HDRGAN [27]	HDR-Trans [24]	SCTNet [34]	SAFNet [20]	DiffHDR [45]	AFUNet [22]	Ours
PU21-PSNR \uparrow	37.62	37.84	40.85	40.68	41.90	40.83	41.60	40.63	42.08	41.95
PU21-SSIM \uparrow	0.9859	0.9862	0.9898	0.9897	0.9913	0.9908	0.9900	0.9896	0.9914	0.9913
LPIPS \downarrow	0.0532	0.0599	0.0461	0.0475	0.0418	0.0392	0.0361	0.0405	0.0398	0.0346
DISTs \downarrow	0.195	0.0221	0.0149	0.0162	0.0132	0.0125	0.0112	0.0115	0.0121	0.0103
MANIQA \uparrow	0.5771	0.5764	0.5791	0.5789	0.5827	0.5821	0.5802	0.5835	0.5806	0.5884
MUSIQ \uparrow	58.98	59.09	59.90	59.84	60.01	59.93	60.09	60.28	60.17	60.81
CLIPIQA \uparrow	0.3841	0.3846	0.4037	0.3932	0.4021	0.4035	0.4089	0.4074	0.4054	0.4211

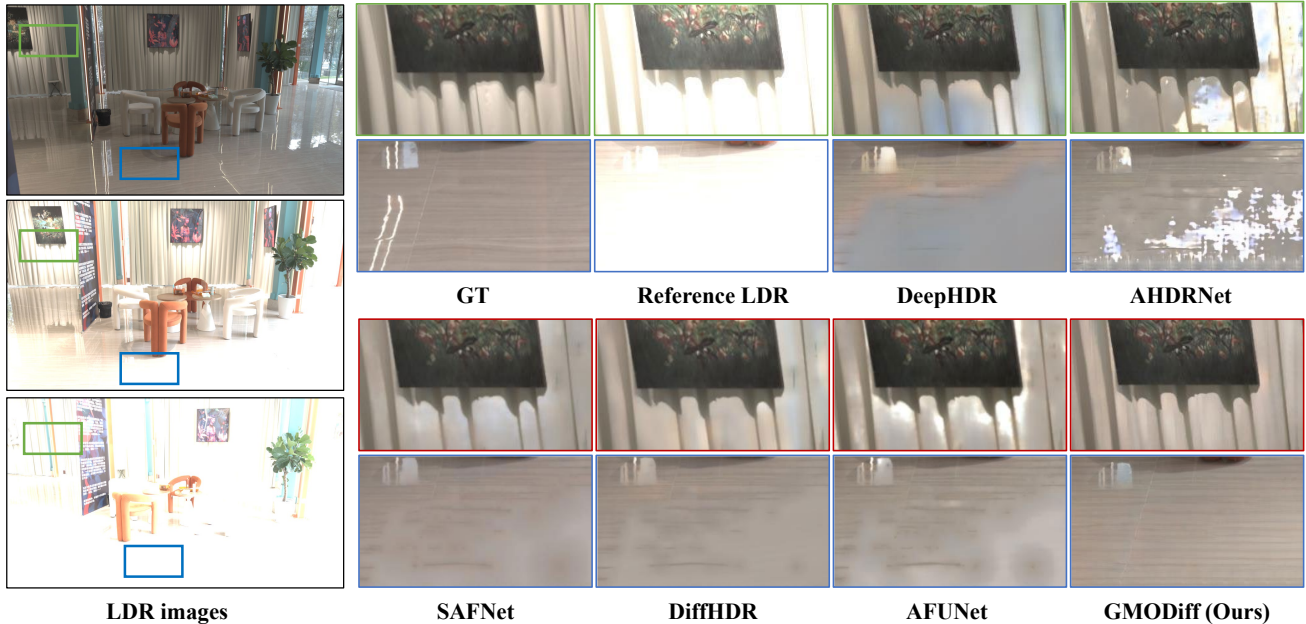


Figure 4. Visual comparisons are conducted on testing data, focusing on zoomed-in local areas of the HDR images estimated by our method and the compared techniques. Our model demonstrates the ability to generate HDR images of superior quality.

of three LDR images captured with exposure levels of either $\{-2, 0, +2\}$ or $\{-3, 0, +3\}$ stops. Notably, Challenge123 [20] also provides static LDR captures for each scene, enabling the generation of five additional training samples per scene compared to the other datasets.

Implementation Details. We implement our model in PyTorch and leverage the `accelerate` library for mixed-precision training with FP16. In stage one, we optimize DaReg using the Adam optimizer with a learning rate of $2e-4$. The training data is preprocessed by extracting 256×256 patches with a stride of 128, and we use a batch size of 16. DaReg adopts the NAFNet architecture [7], with the encoder and decoder comprising $[2, 4, 4, 8]$ and $[2, 2, 2, 2]$ NAFBlocks per stage. The model is trained for 200K iterations on 2 NVIDIA RTX 4090 GPUs. In stage 2, we fine-tune Stable Diffusion 2.1 [30] using LoRa with rank 16. DaReg is frozen and serves as a fixed module. We employ the AdamW optimizer with a learning rate of $5e-5$, weight decay of $1e-10$, and a batch size of 12. This stage is trained

for 300K iterations on 4 NVIDIA RTX 4090 GPUs.

Evaluation Metrics. To ensure fair and comprehensive comparison, we employ both perceptual and distortion-based image quality metrics. For full-reference perceptual evaluation, we use LPIPS and DISTs, which assess perceptual similarity via features from pre-trained deep networks. For no-reference assessment, we adopt MANIQA, MUSIQ, and CLIPIQA, all trained to predict human-perceived quality. In particular, as these metrics are not HDR-specific, we computed them in the tone-mapped domain using a standard μ -law operator. For distortion-based metrics, we include PU-PSNR and PU-SSIM, specifically tailored for HDR images, through the official implementation [3].

4.2. Comparison with SOTA Methods

Compared Methods. We compare GModiff against state-of-the-art CNN- and Transformer-based methods specifically designed for multi-exposure HDR image reconstruction, including DeepHDR [38], NHDRR [42], AH-

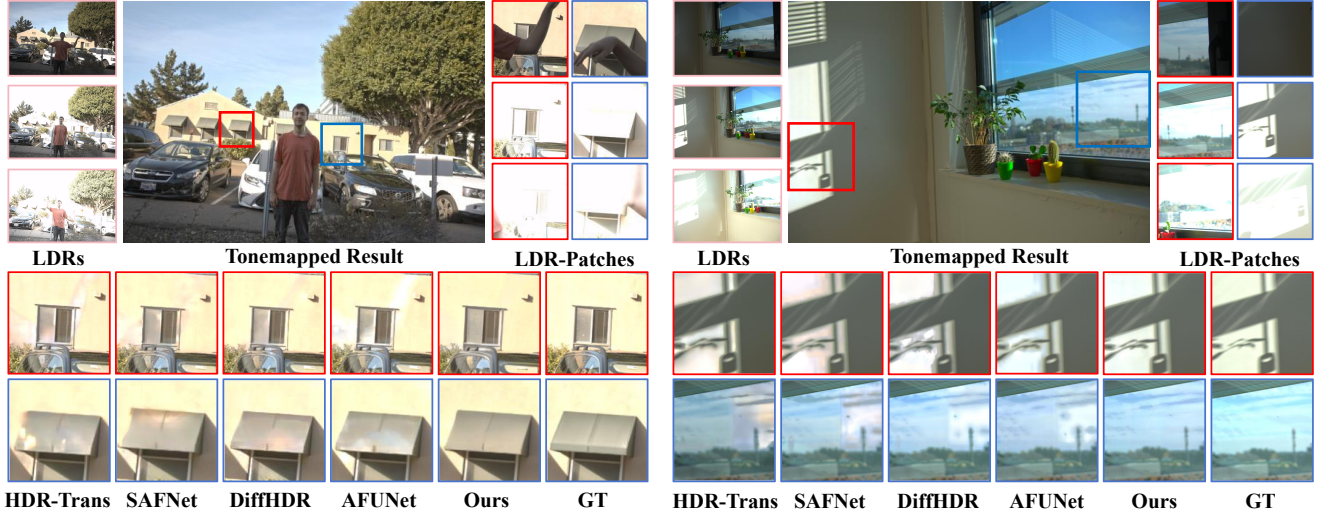


Figure 5. Visual comparisons are conducted on testing data, focusing on zoomed-in local areas of the HDR images estimated by our method and the compared techniques. Our model demonstrates the ability to generate HDR images of superior quality.

DRNet [41], SCTNet [34], and HDR-Trans [24]. In addition, we also evaluate against recent advanced approaches: the GAN-based HDRGAN [27], the diffusion-based DiffHDR [45], the optical-flow-based SAFNet [20], and the deep-unfolding-based AFUNet [22]. For fair comparison, we retrain all these methods on our collected dataset using their official open-source implementations.

Qualitative Results. We present several challenging cases. As shown in Fig. 4, severe camera motion prevents accurate pixel-wise alignment, leaving only semantic cues available to guide reconstruction. The left case of Fig. 5 involves simultaneous human motion and over-saturation, resulting in significant information loss in the input LDR sequence. In the right example of Fig. 5, although the reference frame contains rich visual content, camera motion introduces misalignment that negatively impacts reconstruction quality. It can be observed that existing methods, which directly learn an end-to-end mapping from LDR to HDR, consistently produce noticeable artifacts or ghosting in the aforementioned challenging regions. Although DiffHDR attempts to tackle the ill-posed nature of HDR reconstruction by leveraging the generative capacity of diffusion models, its limited training data prevents it from synthesizing visually plausible results. In contrast, our proposed GMODiff integrates available input cues with strong image priors from pre-trained LDMs to effectively inpaint artifact-prone regions, while avoiding unrealistic hallucinations, resulting in more accurate and perceptually faithful reconstructions.

Quantitative Results. Quantitative comparisons on publicly available datasets are summarized in Tab. 1. Our method consistently outperforms competing approaches across a diverse set of perceptual metrics. Specifically, it achieves notable gains in both full-reference metrics (*e.g.*,

LPIPS and DISTS) and no-reference metrics (*e.g.*, MUSIQ, MANIQA, and CLIPQA), demonstrating its superior ability to reconstruct visually pleasing and perceptually faithful HDR images. Compared to AFUNet [22], the state-of-the-art deep unfold method, our approach attains competitive performance in distortion-based metrics (PU-PSNR and PU-SSIM) while achieving significantly better perceptual quality—highlighting that leveraging regression priors to guide pre-trained latent diffusion models enables an effective trade-off between fidelity and perceptual realism. Moreover, in contrast to diffusion-based alternatives such as DiffHDR [45], our method fully exploits the rich image priors embedded in large-scale pre-trained LDMs. DiffHDR, trained only on limited in-domain data, lacks robust generic priors and struggles in complex real-world scenarios.

4.3. Ablation Studies

Effects of HDR Reconstruction Loss. During the training of GMODiff, we replace the logarithmic compression in Eq. (1), which is non-invertible at zero, with μ -law companding to enable direct supervision using ground-truth HDR images. This modification allows us to reconstruct the HDR image directly from the estimated gain map and apply pixel-wise supervision in the linear HDR domain. As shown in Tab. 2, ablating this reconstruction loss leads to clear performance degradation: minor inaccuracies in gain map estimation are amplified during HDR reconstruction, resulting in reduced fidelity and validating its importance for stable and accurate HDR reconstruction.

Effects of Degradation-Aware Priors. The degradation-aware priors, derived from intermediate features of the first-stage regression branch that predicts a degradation mask, implicitly encode spatially varying artifact patterns. AI-

Table 2. Ablation study of the each component. The best and second best results are colored with red and blue, respectively.

Type	PSNR \uparrow	LPIPS \downarrow	M-IQA \uparrow	MUSIQ \uparrow
DaReg	41.67	0.0432	0.5803	59.77
w/o \mathcal{L}_r	41.54	0.0415	0.5878	60.74
w/o Group Training	42.19	0.0353	0.5848	60.65
w/o c_L	41.76	0.0389	0.5859	60.59
w/o DA Decoder	35.78	0.1076	0.5763	59.89
GMODiff (ours)	41.95	0.0346	0.5884	60.81

Table 3. Inference time comparison on a 1080×1920 image.

Time (s) \downarrow	AHDR	DiffHDR	AFUNet	SCTNet	UltraFusion	Ours
Inference Time	0.24s	13.52s	6.16s	5.66s	93.4s	0.89s

though the mask itself is not used as direct conditioning, its underlying feature representation provides useful cues about input-specific degradation. As shown in Tab. 2, removing these priors leads to a consistent drop across all metrics—both perceptual (*e.g.*, LPIPS, MUSIQ) and distortion-based (*e.g.*, PU-PSNR). This demonstrates that even implicit access to degradation-related features benefits HDR reconstruction, enabling the diffusion model to better adapt to input artifacts and produce more accurate and perceptually plausible results.

Effects of Group Training Strategy. To prevent DaReg from overfitting to the training set, which could hinder GMODiff’s ability to effectively learn artifact removal, we propose a Group Training strategy. As illustrated in Fig. 6, without this strategy, GMODiff can still mitigate degradation in the initial gain map estimation and perform basic artifact correction. However, when Group Training is applied, its artifact removal capability is significantly enhanced, yielding results with nearly imperceptible artifacts. Tab. 2 shows improved perceptual scores with Group Training, while distortion metrics slightly decrease, indicating that Group Training achieves a favorable trade-off between fidelity and perceptual quality.

Effects of DA Decoder. As shown in Tab. 2, removing the DA Decoder leads to a significant drop across all evaluation metrics, especially reference-based ones. This degradation stems from the highly compressed latent space of LDMs, which struggles to preserve fine details. To mitigate this limitation, we inject high-fidelity detail features extracted from intermediate layers of the gain map encoder and selectively refine them using the regression prior obtained from the first stage. As illustrated in Fig. 6, the DA Decoder effectively enhances texture fidelity while suppressing artifacts and ghosting present in the initial gain map. This improvement underscores the critical role of the DA Decoder in recovering high-quality details during HDR reconstruction, thereby substantially boosting the perceptual quality of the final output.

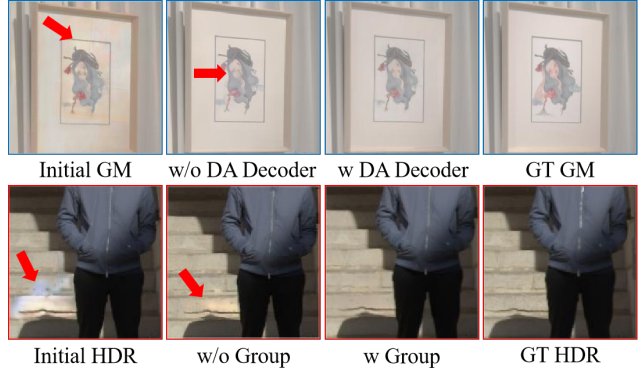


Figure 6. Qualitative results of our ablation study.

4.4. Inference Time Analysis

Tab. 3 compares inference latency on 1920×1080 HDR reconstruction. Our method is overall second-fastest, slightly slower than the lightweight CNN-based AHDR-Net [41], and significantly faster than transformer-heavy models (AFUNet [22], SCTNet [34]), which, despite using efficient window-based attention, incur high latency due to deep stacking of Transformer blocks and processing at high spatial resolutions. Among diffusion-based approaches, UltraFusion [8] requires over a minute per image, owing to patch-wise processing with 50 denoising steps, optical flow alignment, and ControlNet overhead. DiffHDR [45], despite using only 5 steps, operates in pixel space without latent compression, resulting in high memory bandwidth and slow inference. In contrast, our method leverages a pre-trained LDM that performs computation in a highly compressed latent space with a single denoising step, achieving the fastest speed among diffusion-based methods. Moreover, it is compatible with efficient inference frameworks such as xFormers, which further reduce latency through memory, efficient attention and kernel fusion, making it practical for real-world applications.

5. Conclusion

We presented GMODiff, a gain map-driven one-step latent diffusion framework for efficient and high-quality HDR reconstruction from multi-exposure inputs. By formulating HDR reconstruction as gain map refinement in a dual-layer HDR representation, our method can directly exploit pre-trained latent diffusion priors without retraining the VAE or designing HDR-specific latent spaces. A degradation-aware regressor provides a strong initialization and spatial degradation cues, while the one-step latent denoising and degradation-aware decoding jointly suppress ghosting and artifacts. Comprehensive experiments demonstrate that GMODiff outperforms state-of-the-art methods across both perceptual and distortion-based metrics, while significantly reducing inference latency.

References

- [1] Adobe. Gain map specification. <https://helpx.adobe.com/camera-raw/using/gain-map.html>, 2024. Accessed: 2025-11-13. 2
- [2] Apple. Explore hdr rendering with edr. <https://developer.apple.com/videos/play/wwdc2021/10161/>, 2021. Accessed: 2025-11-13. 2, 3
- [3] Maryam Azimi et al. Pu21: A novel perceptually uniform encoding for adapting existing quality metrics for hdr. In *2021 Picture Coding Symposium (PCS)*, pages 1–5. IEEE, 2021. 6
- [4] Luca Bogoni. Extending dynamic range of monochrome and color images through fusion. In *Proceedings 15th International Conference on Pattern Recognition. ICPR-2000*, pages 7–12. IEEE, 2000. 2
- [5] Bin Chen, Gehui Li, Rongyuan Wu, Xindong Zhang, Jie Chen, Jian Zhang, and Lei Zhang. Adversarial diffusion compression for real-world image super-resolution. In *Proceedings of the Computer Vision and Pattern Recognition Conference*, pages 28208–28220, 2025. 2
- [6] Jie Chen, Zaifeng Yang, Tsz Nam Chan, Hui Li, Junhui Hou, and Lap-Pui Chau. Attention-guided progressive neural texture fusion for high dynamic range image restoration. *IEEE Transactions on Image Processing*, 31:2661–2672, 2022. 2
- [7] Liangyu Chen, Xiaojie Chu, Xiangyu Zhang, and Jian Sun. Simple baselines for image restoration. In *European conference on computer vision*, pages 17–33. Springer, 2022. 4, 6
- [8] Zixuan Chen, Yujin Wang, Xin Cai, Zhiyuan You, Zheming Lu, Fan Zhang, Shi Guo, and Tianfan Xue. Ultrafusion: Ultra high dynamic imaging using exposure fusion. In *Proceedings of the Computer Vision and Pattern Recognition Conference*, pages 16111–16121, 2025. 2, 8
- [9] Prafulla Dhariwal and Alexander Nichol. Diffusion models beat gans on image synthesis. *NeurIPS*, 2021. 1
- [10] Yi Du, Zhipeng Zhao, Shaoshu Su, Sharath Golluri, Haoze Zheng, Runmao Yao, and Chen Wang. Superpc: a single diffusion model for point cloud completion, upsampling, denoising, and colorization. In *Proceedings of the Computer Vision and Pattern Recognition Conference*, pages 16953–16964, 2025. 2
- [11] Orazio Gallo, Natasha Gelfandz, Wei-Chao Chen, Marius Tico, and Kari Pulli. Artifact-free high dynamic range imaging. In *2009 IEEE International conference on computational photography (ICCP)*, pages 1–7. IEEE, 2009. 2
- [12] Google. Ultra hdr image format. <https://developer.android.com/media/platform/hdr-image-format>, 2024. Accessed: 2025-11-13. 2, 3, 5
- [13] Yuanshen Guan, Ruikang Xu, Yinuo Liao, Mingde Yao, Lizhi Wang, and Zhiwei Xiong. Hdr image generation via gain map decomposed diffusion. In *Proceedings of the IEEE/CVF International Conference on Computer Vision*, pages 17536–17545, 2025. 1, 2
- [14] Jonathan Ho, Ajay Jain, and Pieter Abbeel. Denoising diffusion probabilistic models. *NeurIPS*, 2020. 1
- [15] Edward J Hu, Yelong Shen, Phillip Wallis, Zeyuan Allen-Zhu, Yuanzhi Li, Shean Wang, Lu Wang, Weizhu Chen, et al. Lora: Low-rank adaptation of large language models. *ICLR*, 1(2):3, 2022. 5
- [16] Jun Hu, O. Gallo, K. Pulli, and Xiaobai Sun. HDR deghosting: How to deal with saturation? In *IEEE Conference on Computer Vision and Pattern Recognition (CVPR)*, pages 1163–1170, 2013. 2
- [17] Tao Hu, Qingsen Yan, Yuankai Qi, and Yanning Zhang. Generating content for hdr deghosting from frequency view. In *Proceedings of the IEEE/CVF Conference on Computer Vision and Pattern Recognition*, pages 25732–25741, 2024. 2
- [18] Nima Khademi Kalantari, Ravi Ramamoorthi, et al. Deep high dynamic range imaging of dynamic scenes. *ACM Trans. Graph.*, 36(4):144–1, 2017. 1, 2, 5
- [19] Sing Bing Kang, Matthew Uyttendaele, Simon Winder, and Richard Szeliski. High dynamic range video. *ACM Transactions on Graphics (TOG)*, 22(3):319–325, 2003. 2
- [20] Lingtong Kong, Bo Li, Yike Xiong, Hao Zhang, Hong Gu, and Jinwei Chen. Safnet: Selective alignment fusion network for efficient hdr imaging. In *European Conference on Computer Vision*, pages 256–273. Springer, 2024. 2, 5, 6, 7
- [21] Guanzhou Lan, Qianli Ma, Yuqi Yang, Zhigang Wang, Dong Wang, Xuelong Li, and Bin Zhao. Efficient diffusion as low light enhancer. In *Proceedings of the Computer Vision and Pattern Recognition Conference*, pages 21277–21286, 2025. 2
- [22] Xinyue Li, Zhangkai Ni, and Wenhan Yang. Afunet: Cross-iterative alignment-fusion synergy for hdr reconstruction via deep unfolding paradigm. *arXiv preprint arXiv:2506.23537*, 2025. 2, 6, 7, 8
- [23] Yinuo Liao, Yuanshen Guan, Ruikang Xu, Jiacheng Li, Shida Sun, and Zhiwei Xiong. Learning gain map for inverse tone mapping. In *The Thirteenth International Conference on Learning Representations*. 2
- [24] Zhen Liu, Yinglong Wang, Bing Zeng, and Shuaicheng Liu. Ghost-free high dynamic range imaging with context-aware transformer. In *European Conference on computer vision*, pages 344–360. Springer, 2022. 1, 2, 4, 6, 7
- [25] Cheng Lu, Yuhao Zhou, Fan Bao, Jianfei Chen, Chongxuan Li, and Jun Zhu. Dpm-solver: A fast ode solver for diffusion probabilistic model sampling in around 10 steps. *Advances in neural information processing systems*, 35:5775–5787, 2022. 2
- [26] Zhangkai Ni, Yang Zhang, Kerui Ren, Wenhan Yang, Hanli Wang, and Sam Kwong. Semantic masking with curriculum learning for robust hdr image reconstruction: Z. ni et al. *International Journal of Computer Vision*, pages 1–16, 2025. 2
- [27] Yuzhen Niu, Jianbin Wu, Wenxi Liu, Wenzhong Guo, and Rynson WH Lau. Hdr-gan: Hdr image reconstruction from multi-exposed ldr images with large motions. *IEEE Transactions on Image Processing*, 30:3885–3896, 2021. 2, 6, 7
- [28] Gaurav Parmar, Taesung Park, Srinivasa Narasimhan, and Jun-Yan Zhu. One-step image translation with text-to-image models. *arXiv preprint arXiv:2403.12036*, 2024. 3
- [29] Dustin Podell, Zion English, Kyle Lacey, Andreas Blattmann, Tim Dockhorn, Jonas Müller, Joe Penna, and

- Robin Rombach. Sdxl: Improving latent diffusion models for high-resolution image synthesis. *arXiv preprint arXiv:2307.01952*, 2023. 1
- [30] Robin Rombach, Andreas Blattmann, Dominik Lorenz, Patrick Esser, and Björn Ommer. High-resolution image synthesis with latent diffusion models. In *Proceedings of the IEEE/CVF conference on computer vision and pattern recognition*, pages 10684–10695, 2022. 6
- [31] Chitwan Saharia, William Chan, Saurabh Saxena, Lala Li, Jay Whang, Emily L Denton, Kamyar Ghasemipour, Raphael Gontijo Lopes, Burcu Karagol Ayan, Tim Salimans, et al. Photorealistic text-to-image diffusion models with deep language understanding. *NeurIPS*, 2022. 1
- [32] Pradeep Sen, Nima Khademi Kalantari, Maziar Yaesoubi, Soheil Darabi, Dan B Goldman, and Eli Shechtman. Robust patch-based hdr reconstruction of dynamic scenes. *ACM Trans. Graph.*, 31(6):203–1, 2012. 2
- [33] Jiaming Song, Chenlin Meng, and Stefano Ermon. Denoising diffusion implicit models. *arXiv preprint arXiv:2010.02502*, 2020. 1, 2
- [34] Steven Tel, Zongwei Wu, Yulun Zhang, Barthélemy Heyrman, Cédric Demonceaux, Radu Timofte, and Dominique Ginhac. Alignment-free hdr deghosting with semantics consistent transformer. *arXiv preprint arXiv:2305.18135*, 2023. 1, 2, 5, 6, 7, 8
- [35] Chao Wang, Zhihao Xia, Thomas Leimkuhler, Karol Myszkowski, and Xuaner Zhang. Lediff: Latent exposure diffusion for hdr generation. In *Proceedings of the Computer Vision and Pattern Recognition Conference*, pages 453–464, 2025. 1, 2, 3
- [36] Lin Wang and Kuk-Jin Yoon. Deep learning for hdr imaging: State-of-the-art and future trends. *IEEE transactions on pattern analysis and machine intelligence*, 44(12):8874–8895, 2021. 1
- [37] Zhengyi Wang, Cheng Lu, Yikai Wang, Fan Bao, Chongxuan Li, Hang Su, and Jun Zhu. Prolificdreamer: High-fidelity and diverse text-to-3d generation with variational score distillation. *Advances in neural information processing systems*, 36: 8406–8441, 2023. 3
- [38] Shangzhe Wu, Jiarui Xu, Yu-Wing Tai, and Chi-Keung Tang. Deep high dynamic range imaging with large foreground motions. In *Proceedings of the European Conference on Computer Vision (ECCV)*, pages 117–132, 2018. 1, 6
- [39] Xinan Xie, Qing Zhang, and Wei-Shi Zheng. Diffusion-based event generation for high-quality image deblurring. In *Proceedings of the Computer Vision and Pattern Recognition Conference*, pages 2194–2203, 2025. 2
- [40] Yanwu Xu, Yang Zhao, Zhisheng Xiao, and Tingbo Hou. Ufogen: You forward once large scale text-to-image generation via diffusion gans. In *Proceedings of the IEEE/CVF Conference on Computer Vision and Pattern Recognition*, pages 8196–8206, 2024. 3, 5
- [41] Qingsen Yan, Dong Gong, Qinfeng Shi, Anton van den Hengel, Chunhua Shen, Ian Reid, and Yanning Zhang. Attention-guided network for ghost-free high dynamic range imaging. In *Proceedings of the IEEE/CVF Conference on Computer Vision and Pattern Recognition*, pages 1751–1760, 2019. 1, 2, 4, 6, 7, 8
- [42] Qingsen Yan, Lei Zhang, Yu Liu, Yu Zhu, Jinqiu Sun, Qinfeng Shi, and Yanning Zhang. Deep hdr imaging via a non-local network. *IEEE Transactions on Image Processing*, 29: 4308–4322, 2020. 6
- [43] Qingsen Yan, Weiye Chen, Song Zhang, Yu Zhu, Jinqiu Sun, and Yanning Zhang. A unified hdr imaging method with pixel and patch level. In *Proceedings of the IEEE/CVF Conference on Computer Vision and Pattern Recognition*, pages 22211–22220, 2023. 1, 2
- [44] Qingsen Yan, Tao Hu, Yuan Sun, Hao Tang, Yu Zhu, Wei Dong, Luc Van Gool, and Yanning Zhang. Towards high-quality hdr deghosting with conditional diffusion models. *IEEE Transactions on Circuits and Systems for Video Technology*, pages 1–1, 2023. 4
- [45] Qingsen Yan, Tao Hu, Yuan Sun, Hao Tang, Yu Zhu, Wei Dong, Luc Van Gool, and Yanning Zhang. Toward high-quality hdr deghosting with conditional diffusion models. *IEEE Transactions on Circuits and Systems for Video Technology*, 34(5):4011–4026, 2023. 2, 6, 7, 8
- [46] Zongsheng Yue, Kang Liao, and Chen Change Loy. Arbitrary-steps image super-resolution via diffusion inversion. In *Proceedings of the Computer Vision and Pattern Recognition Conference*, pages 23153–23163, 2025. 2